Observation of Superheavy Nuclei Produced in the Reaction of ^{86}Kr with ^{208}Pb

V. Ninov,[1] K. E. Gregorich,[1] W. Loveland,[2] A. Ghiorso,[1] D. C. Hoffman,[1,3] D. M. Lee,[1] H. Nitsche,[1,3] W. J. Swiatecki,[1] U. W. Kirbach,[1] C. A. Laue,[1] J. L. Adams,[1,3] J. B. Patin,[1,3] D. A. Shaughnessy,[1,3] D. A. Strellis,[1] and P. A. Wilk[1,3]
[1]*Nuclear Science Division, Lawrence Berkeley National Laboratory, Berkeley, California 94720*
[2]*Department of Chemistry, Oregon State University, Corvallis, Oregon 97331*
[3]*Department of Chemistry, University of California, Berkeley, California 94720*
(Received 27 May 1999)

Following a prediction by Smolańczuk [Phys. Rev. C **59**, 2634 (1999)], we searched for superheavy element formation in the bombardment of ^{208}Pb with 449-MeV ^{86}Kr ions. We have observed three decay chains, each consisting of an implanted heavy atom and six subsequent α decays, correlated in time and position. In these decay chains, a rapid (ms) sequence of high energy α particles ($E_\alpha \geq 10$ MeV) indicates the decay of a new high-Z element. The observed chains are consistent with the formation of $^{293}118$ and its decay by sequential α-particle emission to $^{289}116$, $^{285}114$, $^{281}112$, $^{277}110$, ^{273}Hs ($Z = 108$) and ^{269}Sg ($Z = 106$). The production cross section is $2.2^{+2.6}_{-0.8}$ pb.

PACS numbers: 25.70.Jj, 27.90.+b

The synthesis of new heavy nuclei has fundamental interest for nuclear physics and chemistry. The heaviest nuclei provide a laboratory to test our ideas of nuclear structure at the limits of large numbers of protons in the nucleus. For over 25 years, scientists have sought to find or synthesize superheavy nuclei at or near the region $Z = 114$ and $N = 184$ [1], although some calculations suggest that the region of maximum stability may be near $Z = 120$ or $Z = 126$ [2,3].

The synthesis of elements 110–112 [4–7] and element 114 [8] has invigorated this quest. However, it has proven difficult to proceed beyond element 112 [9] using the so-called "cold fusion" approach [10] of bombarding Pb or Bi target nuclei to produce heavy compound nuclei at low excitation energies. The usual extrapolations of existing data on the synthesis of elements 110–112 indicate that to reach still heavier elements will require orders of magnitude increases in accelerator beam currents and new target technologies.

However, the recent prediction of Smolańczuk [11] indicates that the cold fusion reaction of ^{86}Kr with ^{208}Pb should produce superheavy nuclei ($^{293}118$ and its decay products) with an evaporation residue (EVR) cross section of 670 pb. This would represent a dramatic increase in cross section. His predicted decay sequence [12] for the products of the $^{208}\text{Pb}(^{86}\text{Kr}, n)^{293}118$ reaction is shown in Table I.

We have studied this reaction at the 88-Inch Cyclotron of the Lawrence Berkeley National Laboratory, using the Berkeley gas-filled separator [13]. A schematic diagram of the separator is shown in Fig. 1. A $^{86}\text{Kr}^{19+}$ beam produced with the Advanced Electron Cyclotron Resonance source [14] was accelerated to 459 MeV[ΔE(FWHM) = 2.3 MeV] at an average current of ~300 particle nanoamperes (1.9×10^{12} ions/s). It went through the 0.1 mg/cm^2 carbon entrance window of the separator and struck a ^{208}Pb target placed 0.5 cm downstream from the window. The targets were 300–450 μg/cm^2 thick (sandwiched between 40 μg/cm^2 C on the upstream side and 10 μg/cm^2 C on the downstream side) [15]. Nine of them were mounted on a wheel that was rotated at 400 rpm. The beam energy at the center of the target was 449 MeV [16]. The beam intensity was monitored by two silicon detectors (mounted at ±30 deg with respect to the incident beam) that detected elastically scattered beam particles from the target. During the first experiment (8–12 April 1999), a dose of 0.7×10^{18} ions was delivered to the target and two correlated EVR-α-particle decay chains were observed. During the second experiment (30 April–05 May 1999), a dose of 1.6×10^{18} ions was delivered and one correlated EVR-α-particle decay chain was observed.

The EVRs ($E \sim 131$ MeV) were separated spatially in flight from beam particles and transfer reaction products by their differing magnetic rigidities in the gas-filled separator. The separator consists of three magnets, a vertically focusing quadrupole magnet followed by a strong horizontally focusing gradient dipole magnet and a flat field dipole magnet. The separator is filled with helium gas at a pressure of 1 torr. We have estimated the magnetic rigidity ($B\rho$) to be 2.11 Tm [17]. The optimal magnetic field setting was obtained by scaling the values from the measured focal plane EVR distributions for the

TABLE I. Predicted [12] decay sequence for $^{293}118$.

$^{A}Z_{N}$	Q_α (MeV)	T_α
$^{293}118_{175}$	12.23	31 μs–310 μs
$^{289}116_{173}$	11.37	960 μs–9.6 ms
$^{285}114_{171}$	11.18	800 μs–8.0 ms
$^{281}112_{169}$	11.00	610 μs–6.1 ms
$^{277}110_{167}$	10.77	620 μs–6.2 ms
$^{273}_{108}\text{Hs}_{165}$	9.69	120 ms–1.2 s
$^{269}_{106}\text{Sg}_{163}$	8.35	8.0 min–80 min
$^{265}_{104}\text{Rf}_{161}$	SF	41 min

 0031-9007/99/83(6)/1104(4)$15.00

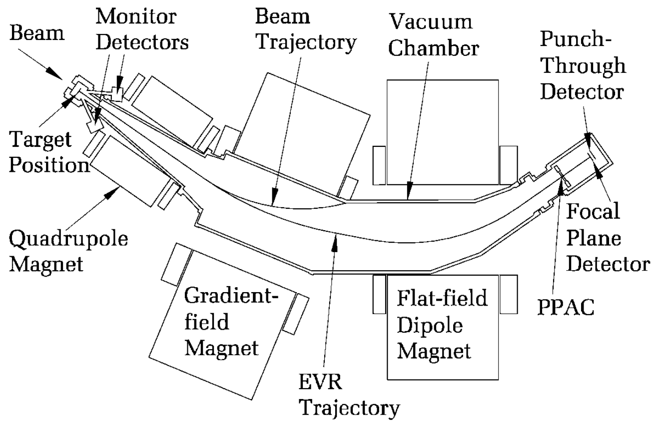

FIG. 1. Schematic diagram of the Berkeley gas-filled separator as configured for this experiment.

analog reaction of 459-MeV ^{86}Kr + ^{116}Cd with estimated $B\rho$ of 1.50 Tm.

The efficiency of the separator for transport and implantation of EVRs was estimated by studying the ^{86}Kr + ^{116}Cd reaction to make α-particle emitting $^{194-198}$Po isotopes. By comparing the measured Po implantation rates with predicted EVR production cross sections [18], we estimate a separator efficiency of ~75%. This efficiency agrees with Monte Carlo simulations of ion trajectories through the separator.

In the focal plane region of the separator, the EVRs passed through a 10 cm × 10 cm parallel plate avalanche counter (PPAC) [19] that recorded the time, ΔE, and x, y positions of the particles. In the first experiment, the PPAC was placed ~3 cm from the focal plane detector while in the second experiment, the PPAC was ~29 cm from the focal plane detector. In the second experiment, the time of flight of the EVRs between the PPAC and the focal plane detector was measured. In both experiments, the PPAC was used to distinguish (99.1% efficiency) between particles hitting the focal plane detector that were beam related and events due to the decay of implanted atoms.

After passing through the PPAC, the recoils were implanted in a 16-strip, 300-μm thick passivated ion implanted silicon detector at the focal plane that had an active area of 80 mm × 35 mm. The strips were position sensitive in the vertical (35 mm) direction. The position resolution along each strip was measured to be 0.58 mm for recoil-α correlations in the ^{86}Kr + ^{116}Cd reaction. The energy response of each strip of the focal plane detector was calibrated using implanted recoils. An average energy resolution of 30 keV for 5–9 MeV α particles was measured for this detector. The focal plane detector had an estimated efficiency of 60% for the detection of full energy 12 MeV α particles following implantation of a ^{293}118 nucleus to a calculated depth of 14 μm. A second silicon strip "punch-through" detector was installed behind this detector to reject particles passing through the primary detector. In the first experiment, a 50 mm × 50 mm detector was used that did not back the entire focal plane detector, while in the second experiment a detector was used that backed the full focal plane detector.

In the first experiment, with a beam current of ~300 particle nanoamperes of ^{86}Kr striking a ^{208}Pb target, the average total counting rate ($E \geq 0.5$ MeV) in the focal plane detector was ~50 s^{-1}. A modification of the beam stop reduced this rate to ~15–20 s^{-1} in the second experiment. The number of particles with energies, $4 \leq E \leq 13$ MeV, was 0.5 s^{-1}. In Fig. 2, the low energy spectrum recorded in the focal plane detector during the entire second experiment is displayed under several conditions. In Fig. 2(a), we show the ungated spectrum.

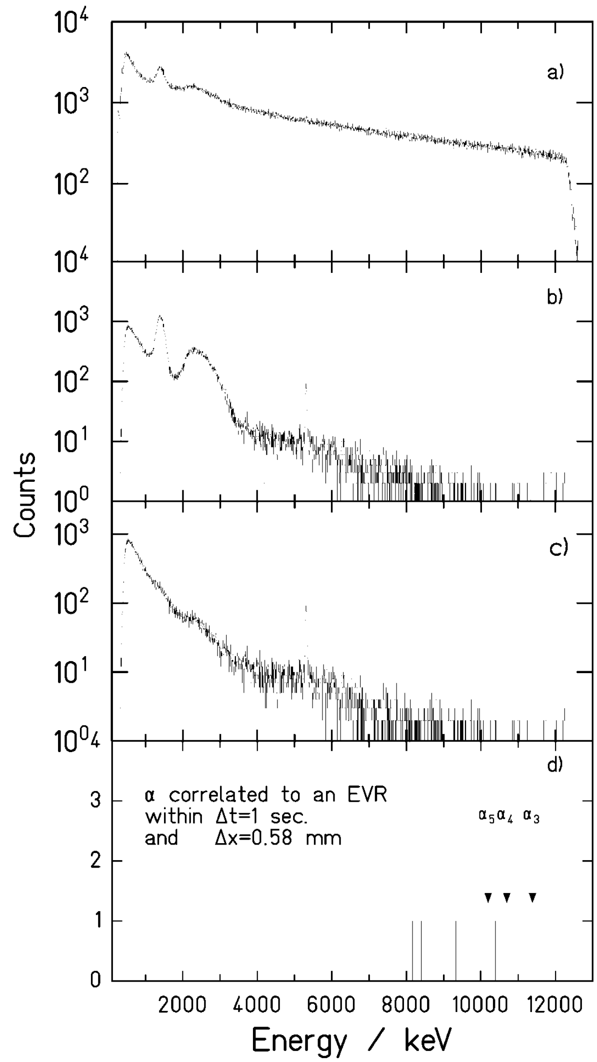

FIG. 2. The α-particle energy spectrum recorded during the entire second experiment. (a) The ungated singles spectrum. (b) The spectrum after applying the PPAC veto. (c) The effect of adding the veto of the punch-through detector to the total veto. (d) The spectrum of all events with $8.1 \leq E \leq 13.0$ MeV correlated in position to an implant, satisfying the veto requirements, which occurred within 1 s of implantation. The arrows indicate members of the decay chain observed in this second experiment.

In Fig. 2(b), the spectrum after applying the PPAC veto is shown. In Fig. 2(c), we display the effect of adding the veto of the "punch-through" detector to the total veto. Finally, in Fig. 2(d), we show the spectrum of all events with $8.1 \leq E \leq 13.0$ MeV satisfying both requirements, which were correlated in position and time (within 1 s) with an implanted recoil. Note that 3 of the 16 counts shown in Fig. 2(d) are part of a single decay chain.

We have observed three decay chains consisting of an implanted heavy atom correlated in position and time with six subsequent α decays for the reaction of 449-MeV ^{86}Kr with ^{208}Pb. This corresponds to a production cross section of $2.2^{+2.6}_{-0.8}$ pb. The observed correlations are shown in Fig. 3 in terms of the predicted decay sequences for ^{293}118. For the third observed chain, we have chosen to indicate the presence of a "missing" α particle. This first α-particle decay could have been missed because it occurred within the 120-μs dead time (after recoil implantation) of the data acquisition system. Based upon the sequences shown in Fig. 3, the half-lives [20] of the decay chain members are ^{293}118, 120^{+180}_{-60} μs; ^{289}116, 600^{+860}_{-300} μs; ^{285}114, 580^{+870}_{-290} μs; ^{281}112, 890^{+1300}_{-450} μs; ^{277}110, $3.0^{+4.7}_{-1.5}$ ms; and ^{273}Hs, $1.2^{+1.7}_{-0.6}$ s. For the first decay chain, the positions (mm) in strip 11 for the implant and subsequent α decays are 13.3, 13.1, 13.2, 13.2, 12.7, 13.2, and 13.1. The positions (mm) for the second chain (strip 9) and the third chain (strip 13) are 3.5, 3.5, 3.0, 3.3, 3.3, 4.0, 3.8, 3.8 and 5.2, 5.2, 5.1, 5.2, 5.0, 5.3, 5.1, respectively. All positions of the members of each chain agree within the uncertainties expected from the calibrations. Given the small number of events in the energy region of interest [Fig. 2(d), the probability of a chance correlation causing these decay chains is negligible. Chance correlations do limit our ability to unambigiously assign correlations involving α decay and fissionlike decays with lifetimes greater than 20 min, i.e., decays at the end of the observed chains.

The energies of the observed α particles and their lifetimes agree remarkably well with the predictions of Smolańczuk [12]. The overall agreement supports the proposed assignments, and there are no known nuclei that exhibit the observed decay pattern. Thus this observation must be taken as evidence for the formation of new nuclei with very high Z. We considered the possibility that the completely fused system deexcited by emitting an α particle or proton instead of a neutron. Statistical model considerations suggest that the ratio of Γ_n/Γ_α would be proportional to $\exp\{-[S_n - (B_\alpha - Q_\alpha)]/T\}$, where S_n is the neutron separation energy, B_α is the Coulomb barrier for α emission, Q_α is the energy released in removing an α particle from the nucleus, and T is the nuclear temperature. Substituting in these relationships appropriate values of the binding energies [12] and barriers [21] gives $\Gamma_n/\Gamma_\alpha \sim 60$ and $\Gamma_n/\Gamma_p \sim 2000$, indicating that neutron emission is the most probable deexcitation path. Since the excitation energy of the completely fused system is 13 MeV [11], emission of two neutrons is energetically forbidden.

In Fig. 4, we compare our measured values of the α-particle energies with the predictions of several modern mass models. The best agreement with our observations is obtained with Smolańczuk's prediction. The finite range droplet model [22] and the Thomas-Fermi model [23] predict appropriate values of the decay energies for the decay of ^{293}118, ^{289}116, and ^{273}Hs ($Z = 108$), but fail for $Z = 106$, and especially, $Z = 114$. The empirical mass model of Liran and Zeldes [24] is not suitable for extrapolation into this region.

We have presented evidence for the first synthesis of new superheavy elements [^{293}118 and its decay products ^{289}116, ^{285}114, ^{281}112, ^{277}110, ^{273}Hs ($Z = 108$) and ^{269}Sg ($Z = 106$)]. Our results show the unexpected viability of the cold fusion approach to the synthesis of superheavy nuclei using projectiles heavier than ^{70}Zn [9]. The production cross section may be explained by the idea of "unshielded fusion" where, with heavier projectiles, the optimal bombarding energy for the $1n$ deexcitation channel is above the Coulomb barrier.

We gratefully acknowledge the operations staff of the 88-Inch Cyclotron for providing intense, steady beams

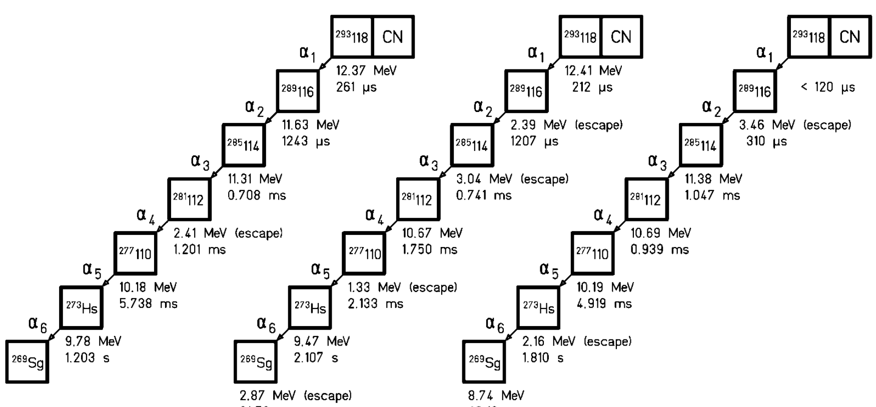

FIG. 3. Observed decay chains for the reaction of 449-MeV ^{86}Kr with ^{208}Pb. The "escape" α particles are those α-particles emitted toward the front of the detector that deposit only a fraction of their energy in the detector.

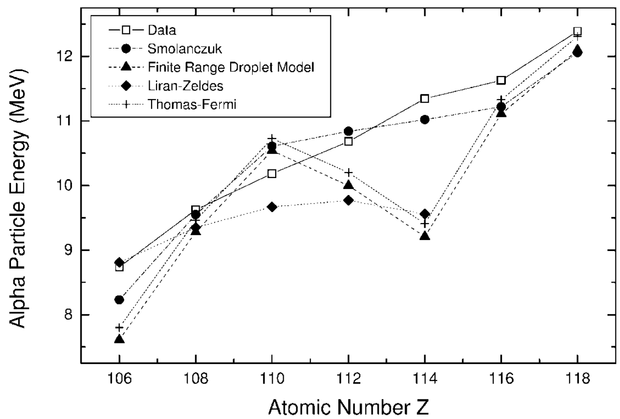

FIG. 4. Comparison of the α-particle energies observed in this work with the predictions of various mass models for the $N - Z = 57$ nuclei.

of ^{86}Kr. We thank B. Lommel and W. Thalheimer of Gesellschaft für Schwerionenforschung for providing the carbon entrance windows and the lead targets. We thank N. Kurz and H. Essel for help in setting up the data acquisition system. We thank G. Münzenberg, S. Hofmann, and F. Hessberger for their support. We gratefully acknowledge R. Smolańczuk for helpful discussions and continuous theoretical support. We thank M. Steiner, J. Yurkon, and D. J. Morrissey at Michigan State University for lending the PPACs. Financial support was provided by the Office of High Energy and Nuclear Physics, Nuclear Physics Division and the Office of Energy Research, Office of Basic Energy Sciences, Chemical Sciences Division of the U.S. Department of Energy, under Contract No. DE-AC03-76SF00098 and Grant No. DE-FG06-88ER40402.

[1] G. T. Seaborg and W. Loveland, *The Elements Beyond Uranium* (Wiley, New York, 1990).
[2] S. Cwiok *et al.*, Nucl. Phys. **A611**, 211 (1996).
[3] K. Rutz *et al.*, Phys. Rev. C **56**, 238 (1997).
[4] A. Ghiorso *et al.*, Nucl. Phys. **A583**, 861c (1995).
[5] S. Hofmann *et al.*, Z. Phys. A **350**, 277 (1995); **350**, 281 (1995).
[6] S. Hofmann *et al.*, Z. Phys. A **354**, 229 (1996).
[7] Yu. A. Lazarev *et al.*, Phys. Rev. C **54**, 620 (1996).
[8] Y. T. Oganessian *et al.*, Lawrence Livermore National Laboratory Report No. UCRL-JC-133388 (to be published); Y. T. Oganessian *et al.*, Nature (London) **400**, 242 (1999).
[9] S. Hofmann and G. Münzenberg, Rev. Mod. Phys. (to be published).
[10] Y. T. Oganessian *et al.*, Nucl. Phys. **A239**, 353 (1975).
[11] R. Smolańczuk, Phys. Rev. C **59**, 2634 (1999).
[12] R. Smolańczuk, Phys. Rev. C **56**, 812 (1997); **60**, 21 301 (1999).
[13] V. Ninov and K. E. Gregorich, *ENAM98,* edited by B. M. Sherrill, D. J. Morrissey, and C. N. Davids (AIP, Woodbury, 1999), p. 704 and http://bgsmc01.lbl.gov/
[14] Z. Q. Xie and C. M. Lyneis, Rev. Sci. Instrum. **67**, 886 (1996).
[15] H. Folger *et al.*, Nucl. Instrum. Methods Phys. Res., Sect. A **362**, 64 (1995).
[16] F. Hubert, R. Bimbot, and H. Gauvin, At. Data Nucl. Data Tables **46**, 1 (1990).
[17] A. Ghiorso *et al.*, Nucl. Instrum. Methods Phys. Res., Sect. A **269**, 192 (1988).
[18] W. Reisdorf, Z. Phys. A **300**, 227 (1981).
[19] D. Swan, J. Yurkon, and D. J. Morrissey, Nucl. Instrum. Methods Phys. Res., Sect. A **348**, 314 (1994).
[20] K. E. Gregorich, Nucl. Instrum. Methods Phys. Res., Sect. A **302**, 135 (1991).
[21] W. E. Parker *et al.*, Phys. Rev. C **44**, 774 (1991).
[22] P. Möller *et al.*, At. Data Nucl. Data Tables **59**, 185 (1995).
[23] W. D. Myers and W. J. Swiatecki, Nucl. Phys. **A601**, 141 (1996).
[24] S. Liran and N. Zeldes, At. Data Nucl. Data Tables **17**, 431 (1976).